


PAPER


Cite this: *RSC Adv.*, 2022, 12, 12607

Synthesis, characterization, *in silico* molecular docking, and antibacterial activities of some new nitrogen-heterocyclic analogues based on a *p*-phenolic unit†

Abdel Haleem M. Hussein,^a Abu-Bakr A. El-Adasy,^a Ahmed M. El-Saghier,^b M. Olish^a and Aboubakr H. Abdelmonsef ^{*c}

Nitrogen-containing heterocycles have shown pharmacological properties against various diseases. Herein, in our study, flavoHB enzyme is a highly promising well-validated target for identification of antibacterial inhibitors using *in silico* and *in vitro* techniques. To identify a new class of antimicrobial agents, *N*-(4-hydroxyphenyl)-3-oxobutanamide was utilized as a precursor in the synthesis of several nitrogen-based heterocycles (pyridine, pyrimidine, and pyrazole) attached to *p*-phenolic substrates 2–8. Treatment of 3-oxobutanamide **1** with malononitrile and/or ethyl cyanoacetate in ethanolic piperidine afforded the pyridinone analogues **2a,b**. On the other hand, treatment of **1** with arylidene cyanothioacetamide furnished the pyridinthione derivative **3**. The reaction of starting material **1** with salicylaldehyde and/or dimethyl formamide dimethyl acetal (DMF-DMA) yielded the pyridinones **4** and **5**, respectively. Reaction of **1** with terephthalaldehyde and urea or thiourea gave bis structures **6a,b**. The reaction of compound **1** with ethyl isothiocyanate and hydrazine hydrate afforded pyrimidine and pyrazole derivatives **7** and **8**, respectively. The structures of newly prepared compounds 2–8 were elucidated using elemental data and spectral analyses such as IR, ¹H NMR, ¹³C NMR, and MS. In addition, an in-house nitrogen-containing heterocycle analogues library 2–8 was examined and screened *in vitro* for their antibacterial effects against Gram-negative bacteria, *Escherichia coli* and Gram-positive bacteria, *Staphylococcus haemolyticus*, *Kocuria kristinae*, *Enterococcus casseliflavus*, and *Bacillus cereus*. Compounds **6a** and **6b** have also shown the highest antibacterial activity against all types of bacteria strains tested except *Kocuria kristinae*. Further, the molecular docking study of the newly prepared compounds with the target enzyme flavohemoglobin (flavoHB) was undertaken to explore their potential inhibitory activities. The results of the docking study indicated that compounds **6a** and **6b** have exerted the highest docking scores against the active site of flavoHB. As a result, the *in vitro* and molecular docking study findings suggested that the compounds **6a** and **6b** (with pyrimidine moiety, amide linkage, and phenolic substrate) might be potent bacterial flavohemoglobin (flavoHB) inhibitors and they could set a promising starting point for future design of antibacterial agents.

Received 19th March 2022
Accepted 18th April 2022

DOI: 10.1039/d2ra01794f

rsc.li/rsc-advances

Introduction

Nitrogen-containing heterocycles^{1–3} such as pyridine, pyrimidine, and pyrazole are important molecular building blocks that are involved in the structural composition of crucial chemicals for humans, including pharmaceuticals, natural resources, veterinary and agricultural products, analytical reagents, and dyes.^{4–6} In addition, nitrogen-based heterocycles attached to

phenolic substrates have received increasing attention due to their pharmacological properties including anticancer, anti-malarial, antimicrobial, and antitubercular⁶ activities. The pursuit of these properties requires efficient synthetic routes that allow rapid construction of diverse aromatic heterocycles with defined substitution patterns. Moreover, N-heterocyclic compounds coupled with the phenolic substrate possess a wide range of medicinal and pharmaceutical activities and are constituents of bioactive molecules such as antibiotics, vitamins, and pharmaceuticals, as represented in Fig. 1. As aforementioned, there are three pharmacophoric features for good antibacterial activity including an N-heterocyclic system, a linker containing a functional group (amide), and an OH group which forms hydrogen bonds, as shown in Fig. 2.

^aChemistry Department, Faculty of Science, Al-Azhar University, Assiut, Egypt

^bChemistry Department, Faculty of Science, Sohag University, 82524 Sohag, Egypt

^cChemistry Department, Faculty of Science, South Valley University, 83523 Qena, Egypt. E-mail: aboubakr.ahmed@sci.svu.edu.eg

† Electronic supplementary information (ESI) available. See <https://doi.org/10.1039/d2ra01794f>

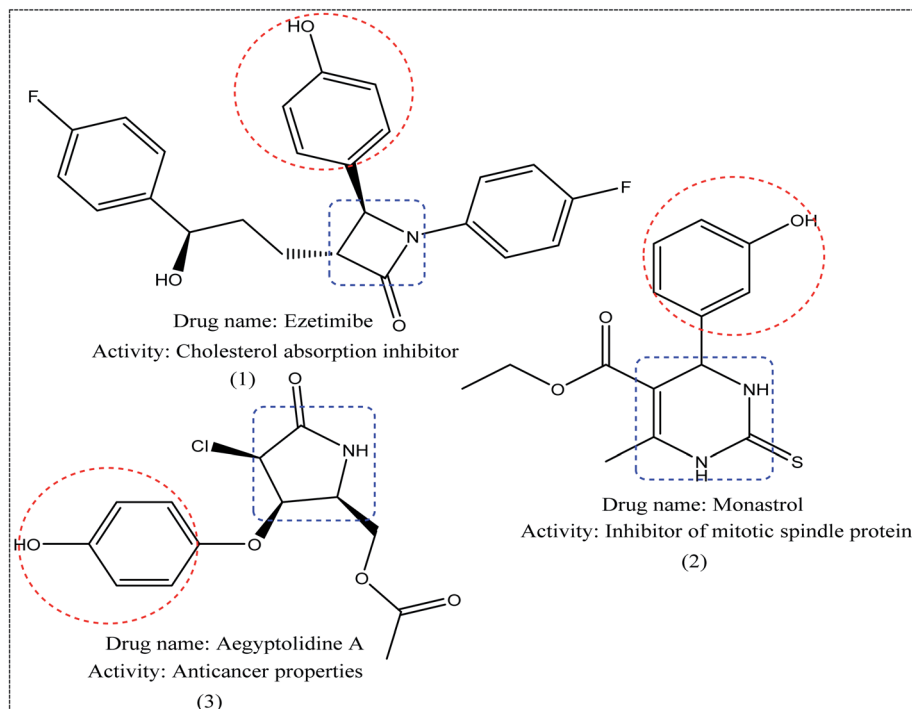



Fig. 1 Examples of N-heterocycles-attached to phenolic moiety as clinical drugs.

On the other hand, Helmick *et al.* reported that nitrogen-containing heterocycles such as azoles had antibacterial activity through inhibition of a bacterial heme-containing enzyme called flavohemoglobin (flavoHB).⁷ The flavohemoglobin is a nitric oxide dioxygenase that used for oxidation of nitric oxide to nitrate.⁸ The function of flavohemoglobin is pivotal for the bacterial survival by protecting bacteria from nitrosative stress.⁹ Thus, flavoHB enzyme has been selected as therapeutic target for identification of antibacterial drug candidates.

In our previous work, we have successfully developed the synthesis of hybrid compounds utilizing 3-oxobutanamide derivatives as starting materials.^{10–16} In light of the above information and as part of our ongoing research in synthesis of

new hybrid molecules with pharmacological interest,^{17–25} herein, an in-house database of nitrogen-containing heterocycle analogues based *p*-phenolic unit was synthesized, characterized and screened *in vitro* for their antibacterial actions against Gram-negative bacteria, *Escherichia coli* (O157:H7), and Gram-positive bacteria, *Staphylococcus haemolyticus* (050402123720221), *Kocuria kristinae* (050032102000201), *Enterococcus casseliflavus* (120200601563571), and *Bacillus cereus* (MH 656790).

Moreover, the molecular docking studies^{26–30} of the newly prepared compounds with the target enzyme flavohemoglobin (flavoHB) were conducted to explore the potential inhibitory activity of these compounds. Finally, ADMET (absorption, distribution, metabolism, excretion, and toxicity) and drug-

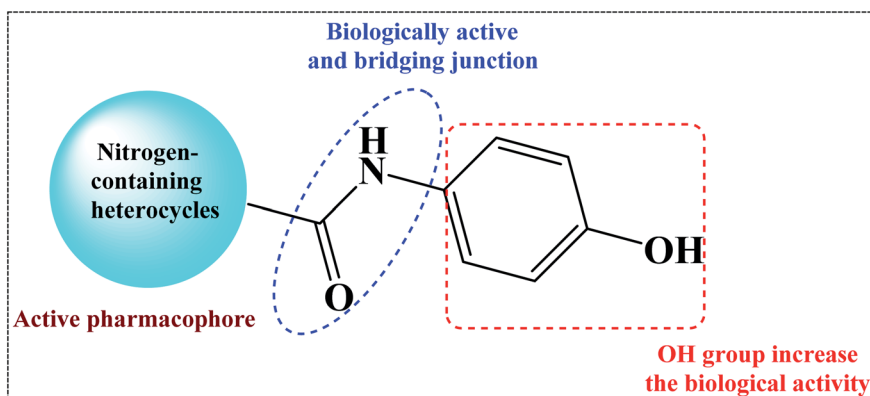


Fig. 2 Design of the target compounds.

likeness predictions of the compounds were calculated using Molinspiration, SwissADME and admetSAR tools. The compounds **6a** and **6b** (with pyrimidine moiety, amide linkage, and phenolic substrate) showed the strongest antibacterial activities, and exhibited the highest binding affinity to the target enzyme flavohemoglobin (flavoHB) with binding energies ΔG_s (-10.4 and -10.0 kcal mol $^{-1}$), respectively, higher than of the standard drug.

Results and discussion

Chemistry

In the current work, treatment of 3-oxobutanamide **1** with active methylene compounds like malononitrile and ethyl cyanoacetate was achieved as represented in Fig. 3. So, treatment of **1** with malononitrile in ethanolic piperidine solution afforded the pyridinone derivative **2a**. IR spectrum of the desired **2a** showed disappearing of acetyl carbonyl and appearance one CN at ν 2194 cm $^{-1}$. ^1H NMR of the structure showed singlet signal at δ 2.40 ppm assigned to CH $_3$, singlet signal for NH $_2$ group appeared at δ 3.73 ppm, singlet signal corresponding to CH-pyridine at δ 7.64 ppm, and OH showed as hump at δ 9.33 ppm. Similarly, the reaction of **1** with ethyl cyanoacetate instead of malononitrile, the reaction takes the way itself not on the ester as expected to give compound **2b**. The IR spectrum of **2b** showed the presence of ester carbonyl band at ν 1721 cm $^{-1}$, amide carbonyl at ν 1635 cm $^{-1}$ and disappearance of CN absorption band. Moreover, ^1H -NMR spectrum revealed a triplet and quartet signals at δ 1.12 and 4.04 ppm for CH $_3$ and CH $_2$ groups of esters, respectively. In addition, the other CH $_3$

group appeared as a singlet at δ 2.28 ppm and appearance of the NH $_2$ protons at δ 5.14 ppm as a singlet, in addition to CH-pyridine at δ 8.12 ppm in interference with the aromatic protons, as well as a singlet signal for OH proton appeared at δ 10.32 ppm.

On the other hand, treatment of compound **1** with benzyldene cyanothioacetamide namely, 2-cyano-3-phenylprop-2-enethioamide furnished the pyridinthione derivative **3**, as shown in Fig. 4. Its IR spectrum showed band at ν 2216 cm $^{-1}$

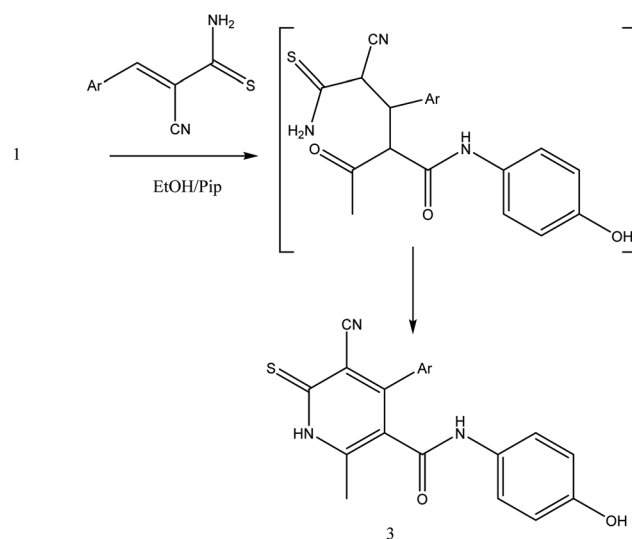


Fig. 4 Synthetic pathway of compound **3**.

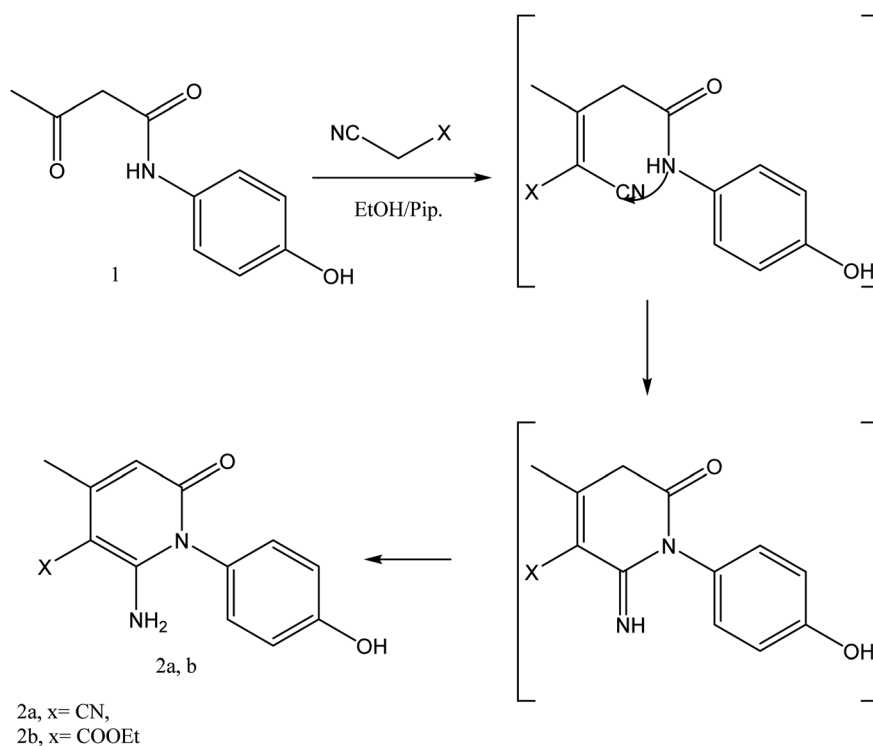


Fig. 3 Synthesis of compounds **2a,b**.

assigned to CN group, and amide carbonyl at ν 1631 cm^{-1} . In addition, ^1H NMR spectrum of compound 3 revealed a singlet signal at δ 1.66 ppm assigned to CH_3 , singlet signal at δ 3.93 ppm assigned to OH group, NH appeared at δ 9.46 ppm and other NH appeared at δ 9.83 ppm.

The reaction of 1 with salicylaldehyde takes the same way too, where the formyl group attacks the active methylene of the starting material to furnish the pyridinone 4, as shown in Fig. 5. The IR spectrum showed ester carbonyl at ν 1707 cm^{-1} and amide carbonyl at ν 1662 cm^{-1} . Moreover, ^1H NMR spectrum showed singlet signal at δ 2.38 ppm assigned to CH_3 , δ 8.88 ppm CH-pyridine appeared and hydroxyl group appeared at δ 9.55 ppm.

During this phase of our research, we have shown that 3-oxobutanamide 1 is expected to react with dimethylformamide-dimethyl acetal (DMF-DMA) in refluxing dry xylene to yield the product which may be enaminone (i) as literature procedure.³¹ But under the reaction conditions we obtained only a product that could be formulated as 5-acetyl-*N*,1-bis(4-hydroxyphenyl)-4-methyl-6-oxo-1,6-dihydropyridine-3-carboxamide 5. However, the spectral data and chemical evidence did not fit this structure. So, the structure (i) was readily ruled out as final product, but it was formed as intermediate based on spectral data. The mass spectrum showed the molecular ion peak at $m/z = 377$

(M^+) corresponding to molecular formula ($\text{C}_{21}\text{H}_{18}\text{N}_2\text{O}_5$). The IR spectrum of compound 5 showed acetyl carbonyl at ν 1710 cm^{-1} , and amide carbonyl at ν 1650 cm^{-1} . ^1H NMR spectrum revealed singlet signal at δ 1.91 ppm referred to acetyl CH_3 , singlet signal at δ 2.18 ppm for other CH_3 , CH-pyridine noted at δ 8.21 ppm, OH appeared as hump at δ 9.50 ppm, and NH appeared at δ 11.46 ppm. Moreover, ^{13}C NMR spectrum revealed two singlet signals assigned for two CH_3 at $\delta = 19.73$ and 21.47 ppm, three singlet signals assigned for carbonyls at δ 164.25, 176.37, 196.46 ppm as declared in Fig. 6.

Formation of compound 5 is assumed to be proceed *via* initial condensation of 3-oxobutanamide 1 with one molecule of DMF-DMA to yield the unstable enaminone (i) which in turn, reacts with another molecule of 1 giving intermediate (ii) by loss NMe_2NH molecule and cyclized to (iii), then loss H_2O to yield 5-acetyl-*N*,1-bis(4-hydroxyphenyl)-4-methyl-6-oxo-1,6-dihydropyridine-3-carboxamide 5.

The reaction of 1 with a mixture of terephthalaldehyde and urea or thiourea afforded the bis-structure 6a,b which confirmed on the bases of its compatible spectroscopic data as represented in Fig. 7. IR spectrum of 6a showed two amide carbonyls at ν 1662 cm^{-1} . ^1H NMR spectrum showed singlet signal at δ 2.28 ppm assigned to CH_3 , singlet signal at δ 5.14 ppm assigned to OH group, singlet signal at δ 9.61

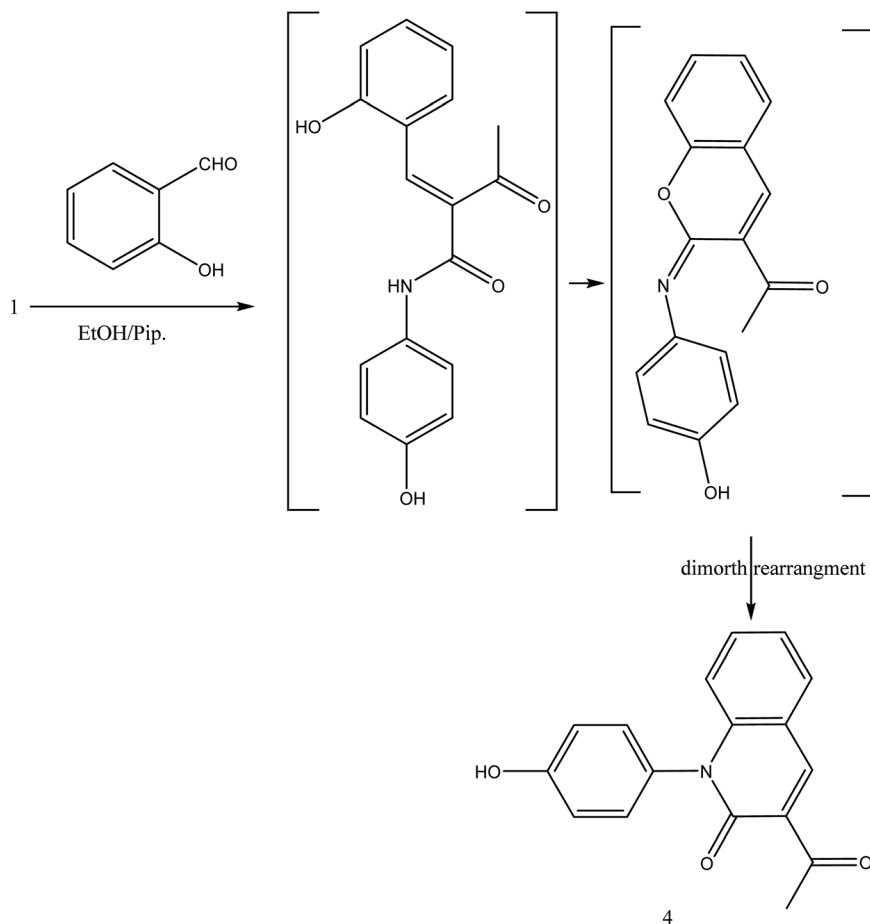


Fig. 5 Synthesis of compound 4.

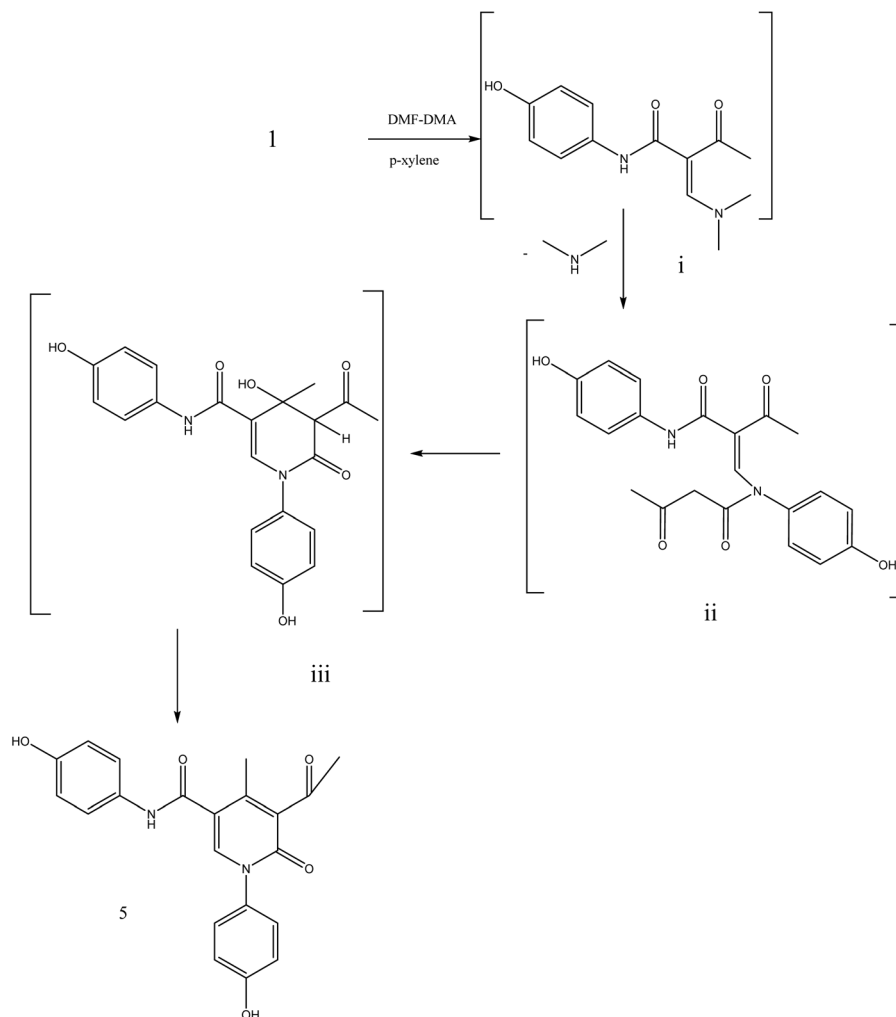


Fig. 6 Synthetic strategy of compound 5.

assigned to NH, and other NH appeared at δ 10.32 ppm. ^{13}C NMR showed singlet signal at δ = 17.62 ppm assigned to CH_3 group and singlet signal at δ = 165.57 ppm assigned to carbonyl group in addition to other carbons in the molecule. Similarly, IR spectrum of compound **6b** showed band at ν 1686 cm^{-1} for amide carbonyl group. ^1H NMR spectrum showed singlet signal at δ 2.33 ppm assigned to CH_3 group, singlet signal at δ 5.29 ppm for OH group, NH amide appeared at δ 8.12 ppm, and NH pyrimidine appeared at δ 10.00 ppm. ^{13}C NMR declared carbonyl at δ = 175 ppm and $\text{C}=\text{S}$ at 192 ppm, and DEPT 135 revealed disappeared of CH_2 signal. Mass spectrum showed molecular ion peak at 595 m/z corresponding to M^{-1} molecular formula $\text{C}_{30}\text{H}_{24}\text{N}_6\text{O}_4\text{S}_2$.

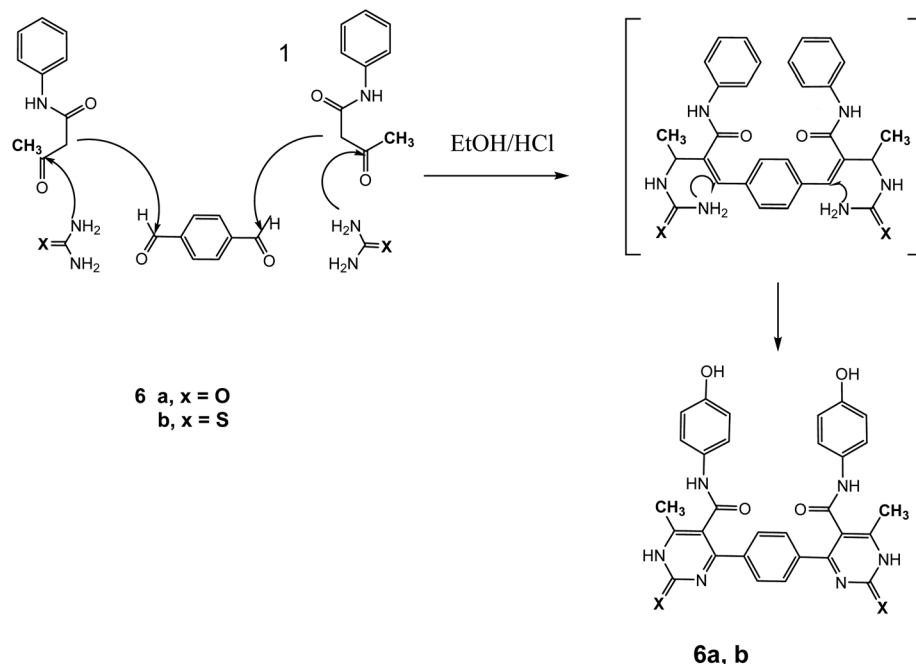
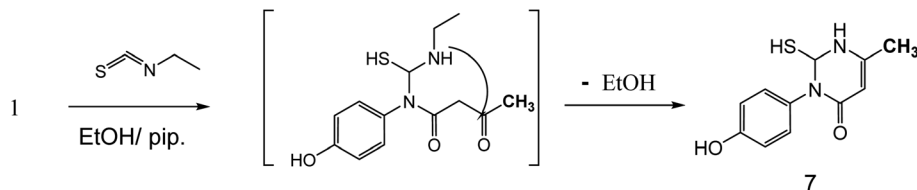
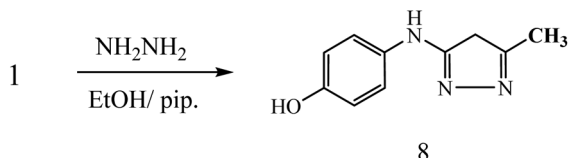
Also, the reaction of 3-oxobutanamide **1** with ethyl isothiocyanate afforded the pyrimidine derivative **7** via attaching firstly on amidic NH not on methylene as expected (Fig. 8). Structure **7** was confirmed by compatible spectroscopic data and elemental analysis. ^1H NMR spectrum of compound **7** showed singlet signal at δ = 1.10 ppm assigned to CH_3 , aromatic protons appeared at δ 6.89–7.27 ppm as doublet of doublet signals, CH-pyrimidine appeared at 9.32 ppm, and broad signals appeared at δ 9.77 and 10.15 ppm referred to SH,

and OH groups, respectively. ^{13}C NMR confirmed the presences of CH_3 signal at δ = 14.82 ppm, and one carbonyl at δ = 165.72 ppm, in addition to other carbons in the structure. Moreover, mass spectrum showed the molecular ion peak at 236 m/z corresponding to molecular formula $\text{C}_{11}\text{H}_{12}\text{N}_2\text{O}_2\text{S}$.

On the other hand, 3-oxobutanamide **1** was treated with hydrazine hydrate to give the pyrazole derivative **8** which confirmed by compatible spectroscopic data and elemental analysis, as declared in Fig. 9. The suggested mechanism for preparation of compound **8** is shown in Fig. 10. The IR spectrum of compound **8** revealed disappearance of two carbonyls. ^1H NMR spectrum showed singlet signal at δ = 2.10 ppm assigned to CH_3 , singlet signal referred to CH_2 at δ = 2.37 ppm, OH group appeared at δ = 5.23 ppm, NH appeared at δ = 5.81 ppm, and doublet of doublet signals at δ = 6.43, and 6.51 ppm referred to four aromatic protons. All spectral data of the prepared compounds are represented in ESI Section as Fig. S1–S21.†

Antibacterial assay

A disc diffusion method (Kirby–Bauer test)³² was used to determine the antimicrobial activity of the newly prepared

Fig. 7 Synthetic pathway of compounds **6a,b**.Fig. 8 Synthetic route of compound **7**.Fig. 9 Synthesis of compound **8**.

compounds **2–8**. Overnight bacterial cultures were diluted to 1 : 10.000 into tryptic soy broth (TSB), by measuring and adjusting the bacterial suspension OD₅₉₅, using spectrophotometer, Spectronic™. Nutrient agar (OXOID) for bacteria was inoculated with microbial cell suspension (200 µL in 20 mL medium), and poured into sterile Petri dishes. Sterile paper discs of 6 mm diameter saturated with tested compound placed on the surface of the inoculated agar plates, the susceptibility testing following the guidelines of the National Committee for Clinical Laboratory Standards.^{33,34} Negative control was done using paper discs loaded with 20 µL of distilled water. Incubate overnight (24 h) at 37 °C. At the end of the incubation period the antibacterial activity was evaluated by measuring the inhibition zones.³⁵

The result presented in Table 1, showed that compounds **6a** and **6b** had the best antibacterial activities close to standard drug against all types of bacteria strains tested except *Kocuria kristinae*. The compounds **4** and **7** had moderate antibacterial activity against Gram-negative bacteria *Staphylococcus haemolyticus*. Finally, compounds **2a,b**, **3**, **5**, and **8** had not any antibacterial activities against any tested bacterial strains (Table 1). The antibacterial activity is shown in the ESI Section, as Fig. S22.†

MIC values showed promising results for most tested compounds as shown in Table 2. Within the tested bacteria, the MIC values were ranged from 0.5 to 2 mg mL⁻¹. Interestingly, both Gram-negative and Gram-positive bacteria were sensitive to the compounds. The antimicrobial activity can be modulated by the presence of pyrimidine moiety, amide linkage, and phenolic substrate.

Computational study

To investigate the affinity and orientation of the newly synthesized molecules against the active site of the target enzyme, an *in silico* study was performed.^{36,37} In the present study, bacterial flavoHB enzyme (PDB: 3OZU)³⁸ has been selected as therapeutic target for identification of antibacterial drug candidates

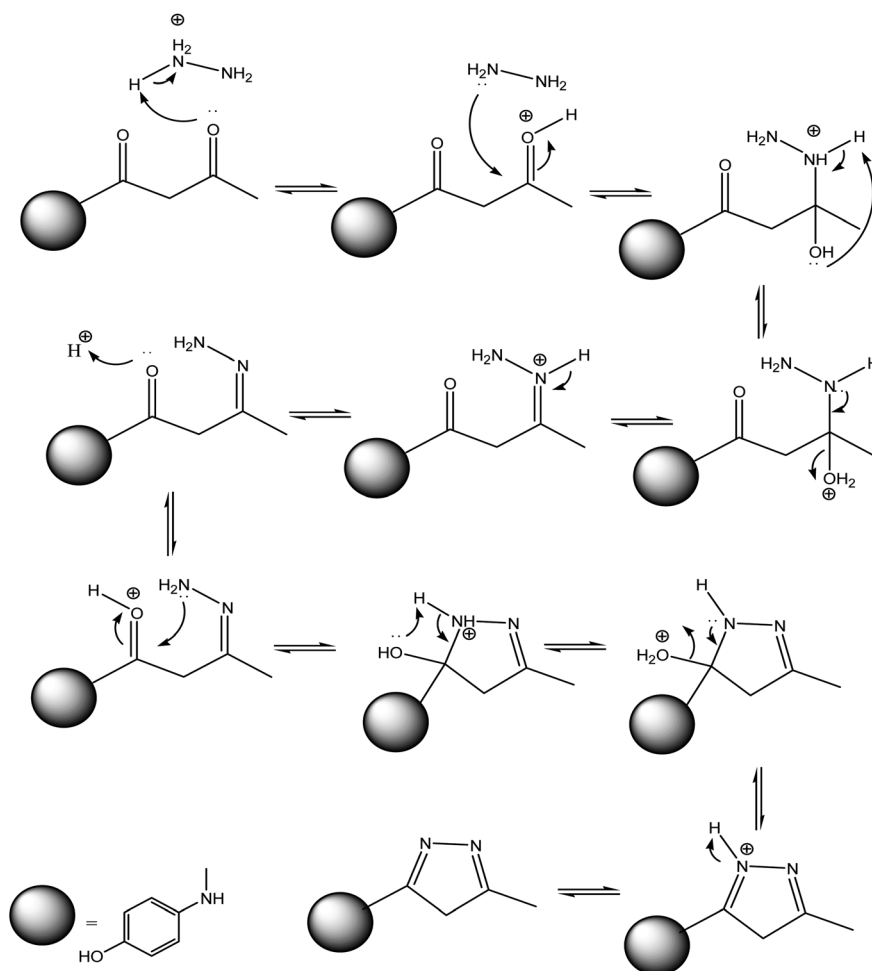


Fig. 10 Suggested mechanism for synthesis of compound 8.

through molecular docking technique. In addition, levofloxacin was selected as a standard drug to compare its binding affinity with those of the docked compounds.

The compounds **6a,b** with the strong antibacterial activities, exhibited the highest binding affinity to the target enzyme with binding energies ΔG_s (-10.4 and -10.0 kcal mol $^{-1}$),

Table 1 Antibacterial activity of the compounds 2–8 and standard drug against the tested bacteria by disc diffusion method (Kirby–Bauer test)^a

Inhibition zone diameters (mm)

Compounds (2.0 mg per disc)	Gram (–ve) bacteria		Gram (+ve) bacteria		
	<i>E. coli</i> (O157:H7)	<i>S. haemolyticus</i> (050402123720221)	<i>K. kristinae</i> (050032102000201)	<i>E. casseliflavus</i> (120200601563571)	<i>B. cereus</i> (MH 656790)
2a	–ve	–ve	–ve	–ve	–ve
2b	–ve	–ve	–ve	ND	1 ± 0.3
3	ND	–ve	–ve	–ve	ND
4	9 ± 1.2	10 ± 0.9	8 ± 0.7	11 ± 1.0	8 ± 0.9
5	3 ± 0.0	ND	–ve	ND	2 ± 0.0
6a	14 ± 1.4	19 ± 1.3	15 ± 1.6	17 ± 1.7	18 ± 0.6
6b	15 ± 0.9	20 ± 1.1	17 ± 1.3	16 ± 0.8	14 ± 0.6
7	12 ± 1.1	8 ± 0.2	11 ± 0.3	6 ± 1.0	8 ± 1.0
8	–ve	2 ± 0.3	ND	1 ± 0.0	–ve
Standard	Levofloxacin (20 mg per disc)				
St. result	17 ± 0.5	21 ± 0.7	20 ± 0.3	20 ± 1.0	16 ± 0.7

^a Abbreviations: –ve: no activity, ND: not determined. Values are mean inhibition zone diameter (mm) ± standard deviation of three replicates.

Table 2 MIC values of compounds 2–8

MIC ^a (mg mL ^{−1})					
Compounds (2.0 mg per disc)	Gram (−ve) bacteria		Gram (+ve) bacteria		
	<i>E. coli</i>	<i>S. haemolyticus</i>	<i>K. kristinae</i>	<i>E. casseliflavus</i>	<i>B. cereus</i>
2a	−ve	−ve	−ve	−ve	−ve
2b	−ve	−ve	−ve	ND	1 ± 0.3
3	ND	−ve	−ve	−ve	ND
4	1.6 ± 0.2	1.4 ± 0.3	1.5 ± 0.3	1.5 ± 0.1	1.6 ± 0.2
5	2.0 ± 0.0	ND	−ve	ND	2.0 ± 0.0
6a	0.9 ± 0.2	0.6 ± 0.3	0.6 ± 0.2	0.7 ± 0.2	0.5 ± 0.1
6b	0.5 ± 0.05	0.3 ± 0.1	0.5 ± 0.1	0.4 ± 0.1	0.4 ± 0.05
7	0.9 ± 0.1	1.2 ± 0.2	1.1 ± 0.3	1.8 ± 0.1	1.5 ± 0.1
8	−ve	2.0 ± 0.3	ND	1.0 ± 0.0	−ve
Standard	Levofloxacin (20 mg per disc)				
St. result	1.6 ± 0.4	2.0 ± 0.2	2.0 ± 0.3	2.5 ± 0.2	2.2 ± 0.3

^a MIC: minimum inhibitory concentration (mg mL^{−1}).

respectively, higher than of the standard drug (Table 3). The compound **6a** engaged to the binding site of the target through three hydrogen bond interactions with the residues Tyr29, and Ala130 at the distances of 2.98, 3.01, and 2.98 Å. While the derivative **6b** docked to the target though one hydrogen bond with Ala130 at 2.95 Å. Compound **2a** interacted with Glu226 of the target enzyme at 2.40 Å, while, derivative **2b** formed two hydrogen bonds and arene–cation interaction with the residues Lys224, Tyr235, and Arg206. On the other hand, compound **3** formed arene-stacked interactions such as arene–arene and arene–cation with Phe43 and Val98 at 5.15, and 3.49 Å, respectively (Table 3). The compound **5** exhibited four HBs and two arene–cation interactions with the amino acid residues Lys84, Gln207, Lys224, Tyr235, and Arg206. Compound **7** with the binding energy ΔG -6.3 kcal mol^{−1}, showed one HB interactions with the residue Asn80. Finally, the docked molecule **8** formed two HB interactions with His392, and Ile391 at the distances 2.96, and 2.34 Å, respectively (Table 2).

On the other hand, the standard drug, levofloxacin exhibited binding energy of -7.9 kcal mol^{−1}, and showed two HBs and one arene–arene interactions with the residues Tyr393 and Glu388 at the distances 3.18, 2.40, and 4.55 Å, respectively (Table 3).

The 2D and 3D representations of the intermolecular interactions between all docked compounds and standard drug with the active site residues of the target enzyme flavoHB are shown in Fig. 11.

Furthermore, the ADMET and drug-likeness results showed interesting values for the compounds (Table 4). All the prepared compounds have molecular weights in the expected range of 130–725 g mol^{−1}. In addition, they have better human intestinal absorption (HIA⁺) score in the range of 66.31–100%, which verified that they could be better absorbed by the human intestine. Further, HBA (H-bond acceptors) and HBD (H-bond donors) satisfy Lipinski's rule of five and were found to be in the acceptable range. The rotatable bonds in the compounds are in limits (1–6). All ligand molecules except **4** and **8** does not

pass the blood–brain barrier that confirming their good CNS safety profile. Finally, all the compounds displayed negative carcinogenicity tests. According to Lipinski's rule of five which states that a molecule violating more than one, it is less likely to be a drug. Therefore, the findings confirmed that the ligand molecules **6a** and **6b** that containing pyrimidine moiety, amide linkage, and phenolic substrate could be used as potent and safe flavoHB inhibitors as promising antibacterial therapeutics.

Materials and methods

Chemistry

All melting points were determined on an electrothermal apparatus and are uncorrected. IR spectra were recorded (KBr discs) on a Shimadzu FT-IR 8201 PC spectrophotometer. ¹H-NMR and ¹³C-NMR spectra (400 MHz) were recorded in DMSO (CD₃)₂SO solution on a BRUKER500 FT-NMR system spectrometer, and chemical shifts are expressed in ppm units using TMS as an internal reference. Mass spectrum was recorded on a GC-MS QP1000 EX Shimadzu. Elemental analyses were carried out at the Microanalytical Center of Cairo University, Egypt.

General procedure for preparation of compounds 2a,b. A mixture of compound **1** (1.93 g, 10 mmol) and malononitrile (0.66 g, 10 mmol) or ethyl cyanoacetate (1.13 g, 10 mmol) was refluxed in ethanol containing few drops of piperidine for 5 h. The reaction mixture was left to cool, then poured onto ice/water containing few drops of conc. HCl. The formed solid product was collected by filtration and recrystallized from ethanol to afford pyridinone derivative **2a,b**.

1-(4-Hydroxyphenyl)-2-imino-4-methyl-6-oxo-1,2,5,6-tetrahydropyridine-3-carbonitrile 2a. Compound **2a** was obtained as brownish crystals, yield (60%), mp = 110–112 °C, IR (KBr) ν cm^{−1}; 3330 (OH), 3207, 2978 (NH₂), 2194 (CN), 1633 (C=O). ¹H NMR (DMSO-*d*₆) (δ ppm); δ_{H} = 2.40 (s, 3H, CH₃), 3.73 (s, 2H, NH₂), 6.46–7.02 (m, 4H, Ar-H), 7.64 (s, 1H, CH-pyridine), 9.33 (hump, 1H, OH). Anal. calcd for C₁₃H₁₁N₃O₂ (241.25): C, 64.72; H, 4.60; N, 17.42%. Found C, 64.45; H, 4.77; N, 17.25.

Table 3 The binding energies of the prepared molecules and their molecular interactions with the active site of the target enzyme

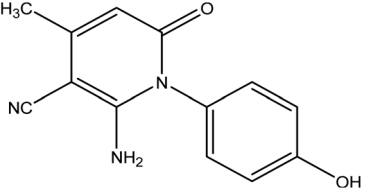
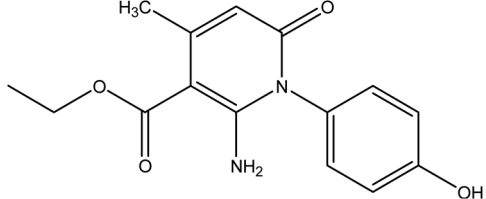
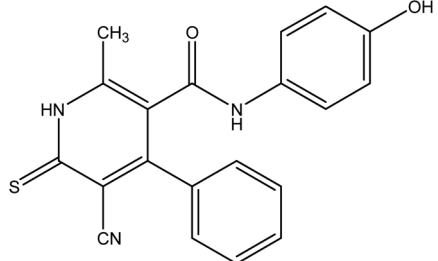
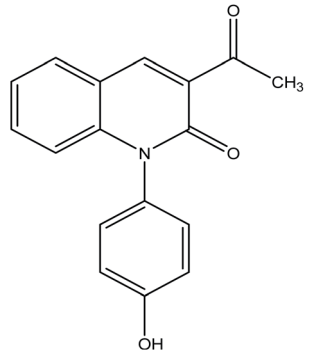
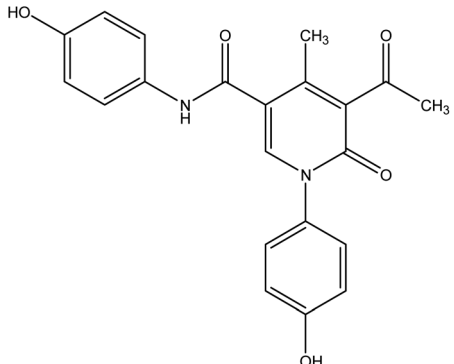
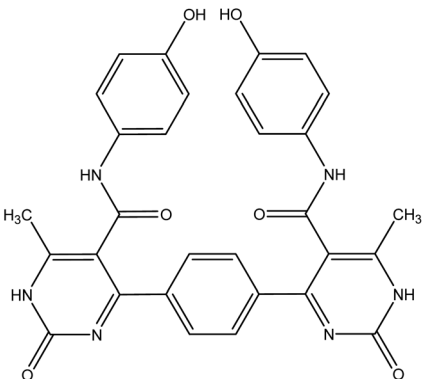
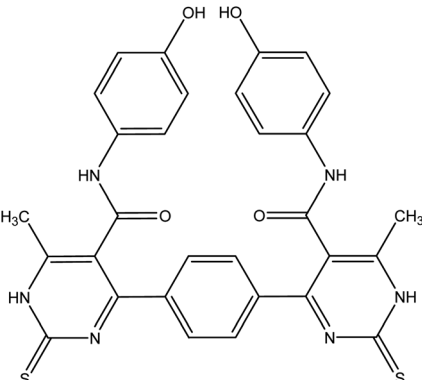
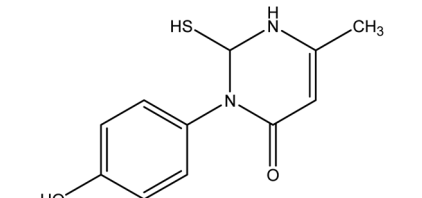
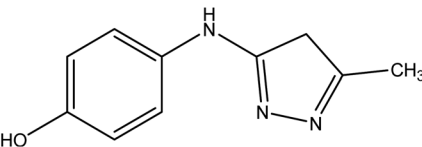
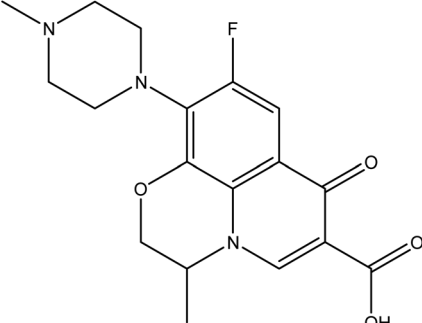
	2D structure	B.E. ^a (kcal mol ⁻¹)	Docked complex (amino acid–ligand) interactions	Distance (Å)
2a		−7.0	H-Bond Glu226:OE2—compound 2a	2.40
2b		−7.1	H-Bond Lys224:N—compound 2b Tyr235:N—compound 2b Arene–cation Arg206:NH2—compound 2b	3.00 2.96 5.13
3		−9.1	Arene–arene Phe43—compound 3 Arene–cation Val98:CG2—compound 3	5.15 3.49
4		−8.1	H-Bond Tyr126:OH—compound 4	2.96
5		−9.6	H-Bond Lys84:NZ—compound 5 Gln207:N—compound 5 Lys224:N—compound 5 Tyr235:N—compound 5 Arene–cation Arg206:NH1—compound 5 Arg206:NH2—compound 5	2.89 2.98 3.00 2.96 4.42 5.98

Table 3 (Contd.)

	2D structure	B.E. ^a (kcal mol ⁻¹)	Docked complex (amino acid–ligand) interactions	Distance (Å)
6a		−10.4	H-Bond Tyr29:OH—compound 6a Tyr29:OH—compound 6a Ala130:N—compound 6a	2.98 3.01 2.98
6b		−10.0	H-Bond Ala130:N—compound 6b	2.95
7		−6.3	H-Bond Asn80:ND2—compound 7	3.08
8		−6.9	H-Bond His392:ND1—compound 8 Ile391:O—compound 8	2.96 2.34
Standard drug		−7.9	H-Bond Tyr393:N—standard drug Glu388:OE1—standard drug Arene–arene Tyr393—standard drug	3.18 2.40 4.55

^a B.E. binding energy.

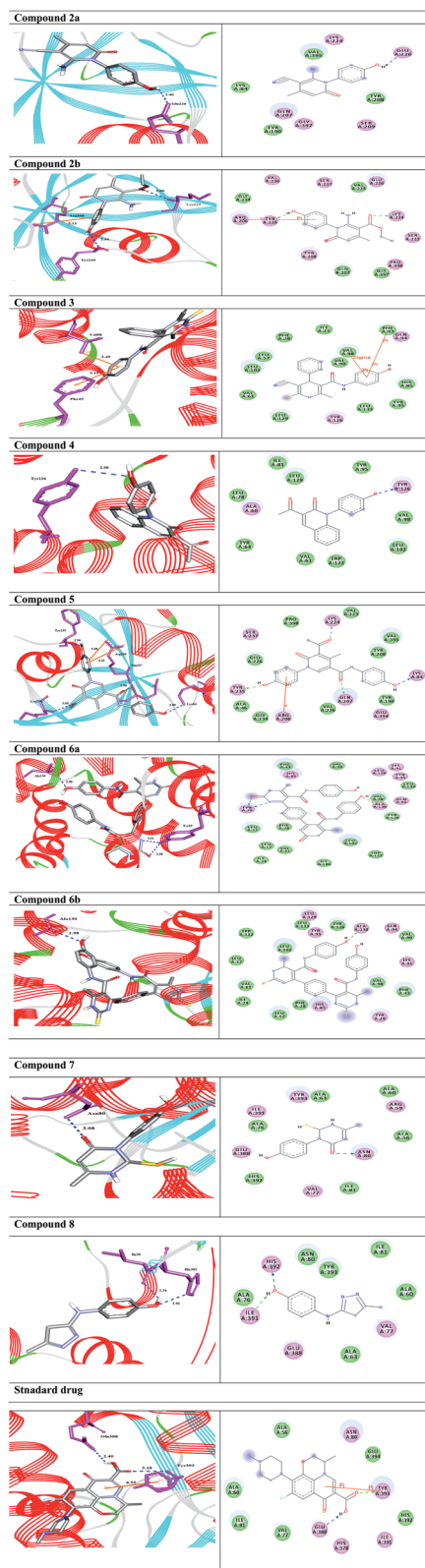


Fig. 11 (Left side) 3D, and (Right side) 2D representations of the docked complexes (compounds and standard drug with the target enzyme). (Left side); H-bonds are represented in blue dotted lines while arene-interactions are shown in orange lines. (Right side); the amino acids are shown in 3 letter code, H-bonds are declared in blue and green dotted lines, while arene-interactions are shown in orange lines.

Ethyl-2-amino-1-(4-hydroxyphenyl)-4-methyl-6-oxo-1,6-dihydropyridine-3-carboxylate **2b**. Compound **2b** was obtained as brown crystals (60%); mp = 129–131 °C; IR (KBr) ν cm⁻¹; 3330 (OH), 3207, 2978 (NH₂), 1722 (C=O), 1636 (C=O-amide). ¹H NMR (DMSO-*d*₆) (δ ppm); δ_{H} = 1.12 (t, 3H, CH₃, *J* = 4 Hz), 2.28 (s, 3H, CH₃), 4.04 (q, 2H, CH₂), 5.14 (s, 2H, NH₂), 6.64–7.92 (m, 4H, Ar-H), 8.12 (s, 1H, CH-pyridine), 10.32 (s, 1H, OH). Anal. calcd for C₁₅H₁₆N₂O₄ (288.30): C, 62.49; H, 5.59; N, 9.72%. Found C, 62.85; H, 5.70; N, 9.40.

4-(4-Chlorophenyl)-5-cyano-N-(4-hydroxyphenyl)-2-methyl-6-thioxo-1,6-dihydro pyridine-3-carboxamide **3**. A mixture of **1** (1.93 g, 10 mmol), and 2-cyano-3-phenylprop-2-enethioamide (1.88 g, 10 mmol), was refluxed in ethanol containing drops of piperidine for 5 h. The reaction mixture was left to cool, then poured onto ice/water containing few drops of conc. HCl. The formed solid product was collected by filtration and recrystallized from ethanol to afford pyridine thiol derivative **3**. Yield (61%), color: dark red crystals, mp = 121–123 °C; IR (KBr) ν cm⁻¹; 3298 (OH), 3193, 3180 (2NH), 2216 (CN), 1631 (C=O). ¹H NMR (DMSO-*d*₆) (δ ppm); δ_{H} = 2.38 (s, 3H, CH₃), 3.93 (s, 1H, NH), 6.45–7.57 (m, 8H, Ar-H), 9.46 (s, 1H, NH-Ph), 9.83 (s, 1H, OH). Anal. calcd for C₂₀H₁₄ClN₃O₂S (395.86): C, 60.68; H, 3.56; Cl, 8.96; N, 10.61; S, 8.10 Found C, 60.71; H, 3.45; Cl, 8.91; N, 10.50; S, 8.27.

3-Acetyl-1-(4-hydroxyphenyl)quinolin-2(1H)-one **4**. A mixture of compound **1** (1.93 g, 10 mmol), and salicylaldehyde (1.22 g, 10 mmol), was refluxed in ethanol containing drops of piperidine for 5 h. The reaction mixture was left to cool, then poured onto ice/water containing few drops of conc. HCl. The formed solid product was collected by filtration and recrystallized from ethyl acetate to yield 3-acetyl-1-(4-hydroxyphenyl) quinolin-2(1H)-one **4**. Yield (96%), color: brown crystals; mp = 105–107 °C; IR (KBr) ν cm⁻¹; 3278 (OH), 1707 (C=O-acetyl), 1662 (C=O-amide). ¹H NMR (DMSO-*d*₆) (δ ppm); δ_{H} = 2.38 (s, 3H, CH₃), 6.85–7.37 (m, 8H, Ar-H), 8.88 (s, 1H, CH-pyridine), 9.55 (s, 1H, OH). Anal. calcd for C₁₇H₁₃NO₃ (279.29): C, 73.11; H, 4.69; N, 5.02. Found C, 73.56; H, 4.65; N, 4.80.

5-Acetyl-N,1-bis(4-hydroxyphenyl)-4-methyl-6-oxo-1,6-dihydropyridine-3-carboxamide **5**. A mixture of 3-oxobutanamide **1** (1.93 g, 10 mmol), and DMF-DMA (1.19 g, 10 mmol), was refluxed in *p*-xylene for 4 h, the solid product formed was filtered off and recrystallized from ethanol to furnish pyridinone derivative **5**. Yield (62%), color: grey crystals, mp = 190–192 °C, IR (KBr) ν cm⁻¹; 3430 (OH) 3231 (NH), 1710 (C=O), 1650 (C=O). ¹H NMR (DMSO-*d*₆) (δ ppm); 1.91 (s, 3H, CH₃), 2.18 (s, 3H, CH₃), 6.69–7.21 (m, 8H, Ar-H), 8.21 (s, 1H, CH-pyridine), 9.50 (hump, 2H, 2OH), 11.46 (s, 1H, NH). ¹³C NMR δ_{C} = 19.73 (CH₃), 21.47 (CH₃), 55.72, 114.48, 115.91, 116.90, 120.70, 121.64, 129.54, 129.75, 132.08, 152.80, 158.64, 164.25 (C=O), 176.37 (C=O), 196.46 (C=O). MS (relative intensity) *m/z*: 377 (M⁻¹, 5%), 245 (10%), 165 (17%), 105 (60%), 44 (100%). Anal. calcd for C₂₁H₁₈N₂O₅ (378.38): C, 66.66; H, 4.79; N, 7.40%. Found C, 66.54; H, 4.60; N, 7.37.

General procedure for preparation of compounds 6a,b. A mixture of three component one pot; 3-oxobutanamide **1** (3.86 g, 20 mmol), terephthalaldehyde (1.35 g, 10 mmol), and urea (1.2 g,

Table 4 Physicochemical and drug-likeness properties of the synthesized compounds 2–8 and the standard drug^a

	Compound 2a	Compound 2b	Compound 3	Compound 4	Compound 5	Compound 6a	Compound 6b	Compound 7	Compound 8	Standard drug
Molecular weight (g mol ⁻¹)	241.25	288.30	361.43	279.30	378.38	564.56	596.69	236.30	189.22	361.37
BBB permeant	No	No	No	Yes	No	No	No	No	Yes	No
% Human intestinal absorption	99.36	84.63	89.53	99.66	93.36	93.76	66.31	92.02	100.00	95.45
(HIA ⁺)										
log <i>p</i>	1.13	1.59	2.91	2.30	1.02	2.28	2.96	1.81	1.66	0.98
HBA	5	6	5	4	7	12	10	4	4	7
HBD	3	3	3	1	3	6	6	2	2	1
N rotatable	1	4	3	2	4	6	6	1	2	2
N violations	0	0	0	0	0	1	1	0	0	0
Volume (Å ³)	212.53	257.00	312.53	247.36	330.74	481.23	498.99	203.85	173.51	311.15
AMES toxicity	Toxic	Nontoxic	Nontoxic	Nontoxic	Nontoxic	Nontoxic	Nontoxic	Nontoxic	Toxic	Nontoxic
Carcinogenicity	Noncarcinogenic	Noncarcinogenic	Noncarcinogenic	Noncarcinogenic	Noncarcinogenic	Noncarcinogenic	Noncarcinogenic	Noncarcinogenic	Noncarcinogenic	Noncarcinogenic
GI absorption	High	High	High	High	High	Low	Low	High	High	High
Bioavailability	0.55	0.55	0.55	0.55	0.55	0.17	0.17	0.55	0.55	0.55
score										

^a Abbreviations and acceptable ranges are as follows; HBA, number of hydrogen bond donors (0.0–6.0); log *p*, logarithm of partition coefficient between *n*-octanol and water (<5); N rotatable, number of rotatable bonds (≤10); TPSA, topological polar surface area (≤140); Mol wt.: (130–725); % (HIA⁺) human oral absorption: >80% high, <25% low; volume: (500–2000).

20 mmol) or thiourea (1.52 g, 20 mmol) was refluxed in ethanol containing drops of hydrochloric acid for 6 h, the solid product formed was filtered off and crystallized from benzene to give pyrimidinone **6a** and thiol derivatives **6b**, respectively.

4,4'-(1,4-Phenylene)bis(N-(4-hydroxyphenyl))-6-methyl-2-oxo-1,2-dihydropyrimidine-5-carboxamide 6a. Compound **6a** was obtained as dark yellow crystals. Yield (50%), mp. = 300–302 °C, IR (KBr) ν cm⁻¹; 3301 (2OH), 3167 (2NH), 3104 (2NH), 1662 (C=O amide). ¹H NMR (DMSO-*d*₆) (δ ppm); δ_{H} = 2.28 (s, 6H, CH₃), 5.14 (s, 2H, OH), 6.64–8.12 (m, 12H, Ar-H), 9.61 (s, 2H, NH-amide), 10.32 (s, 2H, NH-pyrimidine). ¹³C NMR δ_{C} = 17.62, 101.20, 115.40, 127.05, 127.66, 130.41, 143.47, 145.44, 165.57, 174.80. Dept. 135 NMR δ_{C} = (+) 17.61, 115.39, 127.05, 127.66, 130.40, 130.44. Anal. calcd for C₃₀H₂₄N₆O₆ (564.55): C, 63.82; H, 4.28; N, 14.89%. Found C, 63.60; H, 4.19; N, 14.90.

4,4'-(1,4-Phenylene)bis(N-(4-hydroxyphenyl))-6-methyl-2-thioxo-1,2-dihydropyrimidine-5-carboxamide 6b. Compound **6b** was obtained as yellow crystals. Yield (64%), mp = 118–120 °C, yield (64%), color: yellow crystals; mp = 118–120 °C; IR (KBr) ν cm⁻¹; 3221 (OH), 3186 (b, 4NH), 1686 (C=O). ¹H NMR (DMSO-*d*₆) (δ ppm); δ_{H} = 2.33 (s, 6H, CH₃), 5.29 (s, 2H, OH), 6.66–8.12 (m, 12H, Ar-H), 8.12 (s, 2H, NH-amide), 10.00 (s, 2H, NH-pyrimidine). ¹³C NMR δ_{C} = 17.65, 100.69, 115.45, 122.23, 127.64, 130.34, 136.16, 145.98, 150.12, 165.45, 175.09, 192.19. Dept. 135 NMR δ_{C} = (+) 17.66, 54.56, 115.45, 122.23, 127.59, 130.34, 192.91. MS (relative intensity) *m/z*: 596 (M, 0.15%), 368 (M, 0.78%), 304 (M, 9.56%), 275 (M, 10.31%), 134 (M, 29.91%), 105 (M, 47.59%), 57 (M, 100%). Anal. calcd for C₃₀H₂₄N₆O₄S₂ (596.68): C, 60.39; H, 4.05; N, 14.08; S, 10.75%. Found C, 60.70; H, 4.30; N, 14.20; S, 10.70%.

3-(4-Hydroxy-phenyl)-2-mercapto-6-methyl-2,3-dihydro-1H-pyrimidin-4-one 7. A mixture of 3-oxobutanamide **1** (1.93 g, 10 mmol), and ethyl isothiocyanate (0.87 g, 10 mmol), was refluxed in ethanol containing drops of piperidine for 6 h, the formed sticky product precipitated by drops of HCl, then collected by filtration and recrystallized from ethanol to afford pyrimidine derivative **7**. Yield (73%), color: yellow crystals, mp. = 220–222 °C, IR (KBr) ν cm⁻¹; 3300 (OH), 3163 (NH), 1660 (C=O amide). ¹H NMR (DMSO-*d*₆) (δ ppm); δ_{H} = 1.10 (s, 3H, CH₃), 6.89–7.27 (dd, 4H, Ar-H, *J* = 14 Hz), 9.32 (s, 1H, CH-pyrimidine), 9.77 (s, 1H, SH), 10.15 (s, 1H, OH). ¹³C NMR δ_{C} = 14.82, 104.36, 116.19, 116.51, 122.93, 124.74, 126.39, 155.18, 157.61, 165.72. MS (relative intensity) *m/z*: 236 (M⁻¹, 56%), 163 (50%), 151 (49%), 109 (100%). Anal. calcd for C₃₀H₂₄N₆O₆ (236.06): C, 55.91; H, 5.12; N, 11.86; S, 13.57%. Found C, 55.95; H, 5.40; N, 11.90; S, 13.51.

4-((5-Methyl-4H-pyrazol-3-yl)amino)phenol 8. A mixture of compound **1** (1.93 g, 10 mmol), and hydrazine hydrate (0.46 g, 10 mmol), was refluxed in ethanol containing drops of piperidine for 6 h, then the formed solid product was collected by filtration and recrystallized from benzene to yield pyrazole derivative **8**. Yield (78%), color: silver crystals, mp = 144–146 °C; IR (KBr) ν cm⁻¹; 3337 and 3278 (OH, NH). ¹H NMR (DMSO-*d*₆) (δ ppm); δ_{H} = 2.10 (s, 3H, CH₃), 2.37 (s, 2H, CH₂), 5.23 (s, 1H, OH), 5.81 (s, 1H, NH), 6.43–6.51 (dd, 4H, Ar-H, *J* = 24 Hz). Anal. calcd for C₁₀H₁₁N₃O (189.21): C, 63.48; H, 5.86; N, 22.21%. Found C, 63.50; H, 5.99; N, 22.40.

Biological assessment

Compounds **2–8** (2.0 mg per disc), in addition to the standard drug levofloxacin (20 mg per disc) (ready for use discs from Bioanalysis company Turkey, <https://www.bioanalysis.com>) and control dimethyl sulphoxide (DMSO) were tested *in vitro* against pathogenic bacterial strains *Escherichia coli* (O157:H7), *Staphylococcus haemolyticus* (050402123720221), *Kocuria kristinae* (050032102000201), *Enterococcus casseliflavus* (120200601563571), and *Bacillus cereus* (MH 656790) (identified in Al-Azhar University, center of mycology and the regional biotechnology – by using BIOMERIEUX VITEK2 SYSTEM-bio number), as shown in the ESI as Fig. S23.†

Determination of the minimum inhibitory concentration (MIC)

The determination of MIC was assayed as described earlier by Salem *et al.*³⁹ The freshly prepared cultures of both Gram-negative bacteria and/or Gram-positive bacteria were adjusted to OD₅₉₅ of 0.001. 100 μ L of each isolate culture was put into sterilized 96-well plates. Then 20 μ L of the screened compounds (2 mg mL⁻¹) (serial dilutions of 10⁻¹ to 10⁻¹⁰ were used, 8 replicates were made for each dilution into complete raw of the 96-well plate). In addition, levofloxacin (20 mg per disc) was used as reference drug. The un-inoculated media tested as negative control, after 24 h incubation at 37 °C. MIC was determined by the addition of 40 μ L of *p*-iodonitrotetrazolium violet chloride (INT) (0.2 μ g mL⁻¹, Sigma-Aldrich) to the plates and re-incubated at 37 °C for 30 min., the lowest concentration which banned color change is the MIC.⁴⁰

In silico docking approach

Molecular docking study^{41,42} of ligand molecules was carried out to evaluate their binding geometries with the target enzyme flavoHB. To understand the binding mode of interactions of newly synthesized compounds with the target, the crystallographic structure of the enzyme was downloaded from the Protein Data Bank (PDB: 3OZU).³⁸ Additionally, the 2D structures of the ligand molecules were sketched using ChemDraw 16, and converted to SDF format using Open Babel GUI.⁴³ The docking approach was carried out using PyRx-virtual screening tool.⁴⁴ To obtain the 2D and 3D intermolecular representations of the docked compounds, the discovery studio 3.5 was employed. Moreover, *in silico* ADMET and drug-likeness prediction of the molecules were performed using admetSAR, mol inspiration, and SwissADME free accessible tools.

Conclusion

Novel series of nitrogen-based heterocycles attached to *p*-phenolic unit was synthesized. *In vitro* study showed that compounds **6a** and **6b** had appreciable antibacterial activities close to standard drug against all types of bacteria strains tested. Consequently, *in silico* study revealed that compounds **6a** and **6b** showed good binding energies against the target enzyme. Overall; the findings exhibited that compounds **6a** and

6b represent promising starting points for the development of novel antibacterial inhibitors.

Data availability

The original contributions presented in the study are included in the article/ESI;† further inquiries can be directed to the corresponding author.

Author contributions

All authors made a significant contribution to the work reported, whether that is in the conception, study design, execution, acquisition of data, analysis, and interpretation, or in all these areas; took part in drafting, revising or critically reviewing the article; gave final approval of the version to be published; have agreed on the journal to which the article has been submitted; and agree to be accountable for all aspects of the work.

Conflicts of interest

The authors declare no conflict of interest.

References

- 1 S. Shahzad, *et al.*, Folic acid-sulfonamide conjugates as antibacterial agents: Design, synthesis and molecular docking studies, *RSC Adv.*, 2020, **10**, 42983–42992.
- 2 M. Imran, *et al.*, Identification of novel bacterial urease inhibitors through molecular shape and structure based virtual screening approaches, *RSC Adv.*, 2020, **10**, 16061–16070.
- 3 M. Ahmed, M. A. Qadir, A. Hameed, M. Imran and M. Muddassar, Screening of curcumin-derived isoxazole, pyrazoles, and pyrimidines for their anti-inflammatory, antinociceptive, and cyclooxygenase-2 inhibition, *Chem. Biol. Drug Des.*, 2018, **91**, 338–343.
- 4 K. D. Lang, R. Kaur, R. Arora, B. Saini and S. Arora, Nitrogen-Containing Heterocycles as Anticancer Agents: An Overview, *Anti-Cancer Agents Med. Chem.*, 2020, **20**, 2150–2168.
- 5 M. M. Heravi and V. Zadsirjan, Prescribed drugs containing nitrogen heterocycles: an overview, *RSC Adv.*, 2020, **10**, 44247–44311.
- 6 N. Kerru, L. Gummidi, S. Maddila, K. K. Gangu and S. B. Jonnalagadda, A review on recent advances in nitrogen-containing molecules and their biological applications, *Molecules*, 2020, **25**(8), 1909.
- 7 R. A. Helmick, *et al.*, Imidazole antibiotics inhibit the nitric oxide dioxygenase function of microbial flavohemoglobin, *Antimicrob. Agents Chemother.*, 2005, **49**, 1837–1843.
- 8 S. Sari, *et al.*, Azoles containing naphthalene with activity against Gram-positive bacteria: *in vitro* studies and *in silico* predictions for flavohemoglobin inhibition, *J. Biomol. Struct. Dyn.*, 2021, 1–10.
- 9 R. K. Poole, Flavohaemoglobin: the pre-eminent nitric oxide-detoxifying machine of microorganisms, *F1000Research*, 2020, vol. 9, F1000 Faculty Rev-7.
- 10 A. M. Hussein, A. A. Harb and I. A. Mousa, β -oxoanilides in heterocyclic synthesis: An expeditious synthesis of new polyfunctionally substituted pyridine and pyrazole derivatives, *J. Heterocycl. Chem.*, 2008, **45**, 1819–1823.
- 11 M. Abdel-rady, M. I. A. Hassan, M. A. Abou-salim and Y. A. M. M. Elshaier, Multifunctional Isosteric Pyridine Analogs-Based 2-Aminothiazole: Design, Synthesis, and Potential Phosphodiesterase-5 Inhibitory Activity, *Molecules*, 2021, **26**, 1–19.
- 12 M. Abdel-Rady, *et al.*, Functionally substituted arylhydrazones as building blocks in heterocyclic synthesis: Facile synthesis of pyrazoles, triazoles, triazines and quantum chemical studies, *Synth. Commun.*, 2021, **51**, 3099–3115.
- 13 S. A.-M. A. Altaheel, A. A. Khames, A.-B. A. M. El-Adasy, A. M. A. Hassane and A.-H. M. Hussein, 3-Oxobutanamides in Heterocyclic Synthesis: Synthesis, Antimicrobial and Antioxidant Activity of Pyridine, Thiophene, Diazepine and Thiazole Derivatives, *Am. J. Heterocycl. Chem.*, 2021, **7**, 26–32.
- 14 A. H. M. Hussein, M. A. M. Gad-Elkareem, A.-B. A. A. M. El-Adasy, A. A. Khames and I. M. M. Othman, β -Oxoanilides in Heterocyclic Synthesis: Synthesis and Antimicrobial Activity of Pyridines, Pyrans, Pyrimidines and Azolo, Azinopyrimidines Incorporating Antipyrine Moiety, *Int. J. Org. Chem.*, 2012, **02**, 341–351.
- 15 A. H. M. Hussein, *et al.*, Design, synthesis and biological evaluation of new 2-aminothiazole scaffolds as phosphodiesterase type 5 regulators and COX-1/COX-2 inhibitors, *RSC Adv.*, 2020, **10**, 29723–29736.
- 16 A. H. M. Hussein, A.-B. A. El-Adasy, A. A. Khames, A. A. Atalla and M. Abdel-Rady, 3-Oxobutanamides in Heterocyclic Synthesis, Synthesis Approaches for new Pyridines, Pyrimidines and their Fused Derivatives, *ChemistrySelect*, 2017, **2**, 1625–1629.
- 17 A. M. Abo-Bakr, H. M. Alsoghier and A. H. Abdelmonsef, Molecular docking, modeling, semiempirical calculations studies and *in vitro* evaluation of new synthesized pyrimidin-imide derivatives, *J. Mol. Struct.*, 2022, **1249**, 131548.
- 18 A. A. Noser, M. El-Naggar, T. Donia and A. H. Abdelmonsef, Synthesis, *In Silico* and *In Vitro* Assessment of New Quinazolinones as Anticancer Agents via Potential AKT Inhibition, *Molecules*, 2020, **25**, 4780.
- 19 A. A. Noser, A. H. Abdelmonsef, M. El-naggar and M. M. Salem, New Amino Acid Schiff Bases as Anticancer Agents via Potential Mitochondrial Complex I-Associated Hexokinase Inhibition and Targeting AMP-Protein Kinases/mTOR Signaling Pathway, *Molecules*, 2021, **26**, 1–27.
- 20 A. M. El-Saghier, *et al.*, Eco-Friendly Synthesis, Biological Evaluation, and *In Silico* Molecular Docking Approach of Some New Quinoline Derivatives as Potential Antioxidant and Antibacterial Agents, *Front. Chem.*, 2021, **9**, 1–14.
- 21 S. M. Gomha, *et al.*, Thiazole-Based Thiosemicarbazones: Synthesis, Cytotoxicity Evaluation and Molecular Docking Study, *Drug Des., Dev. Ther.*, 2021, **2021**, 659–677.

- 22 A. Haredi Abdelmonsef, M. Eldeeb Mohamed, M. El-Naggar, H. Temairk and A. Mohamed Mosallam, Novel Quinazolin-2,4-Dione Hybrid Molecules as Possible Inhibitors Against Malaria: Synthesis and *in silico* Molecular Docking Studies, *Front. Mol. Biosci.*, 2020, **7**, 105.
- 23 H. R. M. Rashdan, I. A. Shehadi and A. H. Abdelmonsef, Synthesis, Anticancer Evaluation, Computer-Aided Docking Studies, and ADMET Prediction of 1,2,3-Triazolyl-Pyridine Hybrids as Human Aurora B Kinase Inhibitors, *ACS Omega*, 2021, **6**, 1445–1455.
- 24 H. R. M. Rashdan, M. El-Naggar and A. H. Abdelmonsef, Synthesis, molecular docking studies and *in silico* admet screening of new heterocycles linked thiazole conjugates as potent anti-hepatic cancer agents, *Molecules*, 2021, **26**, 1–17.
- 25 H. R. M. Rashdan, *et al.*, Synthesis, Molecular Docking Screening and Anti-Proliferative Potency Evaluation of Some New Imidazo[2,1-*b*]Thiazole Linked Thiadiazole Conjugates, *Molecules*, 2020, **25**, 4997.
- 26 A. El-Maghraby and A. Abdelmonsef, Synthesis, characterization and *insilico* molecular docking studies of novel chromene derivatives as Rab23 inhibitors, *Egypt. J. Chem.*, 2020, **63**(4), 1341–1358.
- 27 R. Rondla, *et al.*, Selective ATP competitive leads of CDK4: Discovery by 3D-QSAR pharmacophore mapping and molecular docking approach, *Comput. Biol. Chem.*, 2017, **71**, 224–229.
- 28 A. H. Abdelmonsef and A. M. Mosallam, Synthesis, *in vitro* biological evaluation and *in silico* docking studies of new quinazolin-2,4-dione analogues as possible anticarcinoma agents, *J. Heterocycl. Chem.*, 2020, **57**, 1637–1654.
- 29 T. Dasari, *et al.*, Design of novel lead molecules against RhoG protein as cancer target – a computational study, *J. Biomol. Struct. Dyn.*, 2017, **35**, 3119–3139.
- 30 A. H. Abdelmonsef, Computer-aided identification of lung cancer inhibitors through homology modeling and virtual screening, *Egypt. J. Med. Hum. Genet.*, 2019, **20**, 1–14.
- 31 L. Kralj, A. Hvala, J. Svete, L. Golič and B. Stanovnik, Aminoacids in the synthesis of heterocyclic systems. The synthesis of methyl 2-acetylaminopropenoate and 2-(N-methyl-N-trifluoroacetyl)amino-3-dimethylaminopropenoate and their application in the synthesis of heterocyclic compounds, *J. Heterocycl. Chem.*, 1997, **34**, 247–255.
- 32 A. W. Bauer, W. M. M. Kirby, J. C. Sherris and M. Turck, Antibiotic Susceptibility Testing by a Standardized Single Disk Method, *Am. J. Clin. Pathol.*, 1966, **45**, 493–496.
- 33 J. A. Kiehlbauch, *et al.*, Use of the National Committee for Clinical Laboratory Standards guidelines for disk diffusion susceptibility testing in New York State Laboratories, *J. Clin. Microbiol.*, 2000, **38**, 3341–3348.
- 34 NCCLS: Standardization in Clinical Laboratory Automation and Information Systems, *JALA J. Assoc. Lab. Autom.*, 1998, **3**(3), 41–42.
- 35 M. Balouiri, M. Sadiki and S. K. Ibnsouda, Methods for *in vitro* evaluating antimicrobial activity: A review, *J. Pharm. Anal.*, 2016, **6**, 71–79.
- 36 A. H. Abdelmonsef, *et al.*, A search for antiinflammatory therapies: Synthesis, *in silico* investigation of the mode of action, and *in vitro* analyses of new quinazolin-2,4-dione derivatives targeting phosphodiesterase-4 enzyme, *J. Heterocycl. Chem.*, 2021, **1**, 1–19.
- 37 A. H. Abdelmonsef, M. A. Abdelhakeem, A. M. Mosallam, H. Temairk, M. El-Naggar, H. Okasha and H. R. M. Rashdan, A search for antiinflammatory therapies: Synthesis, *in silico* investigation of the mode of action, and *in vitro* analyses of new quinazolin-2,4-dione derivatives targeting phosphodiesterase-4 enzyme, *J. Heterocycl. Chem.*, 2022, **59**(3), 474–492.
- 38 H. M. Berman, *et al.*, The protein data bank, *Nucleic Acids Res.*, 2000, **28**, 235–242.
- 39 W. M. Salem, D. M. W. Shibab El-hamed, W. F. Sayed and R. B. Elamary, Alterations in virulence and antibiotic resistant genes of multidrug-resistant *Salmonella* serovars isolated from poultry: The bactericidal efficacy of *Allium sativum*, *Microb. Pathog.*, 2017, **108**, 91–100.
- 40 J. N. Eloff, A sensitive and quick microplate method to determine the minimal inhibitory concentration of plant extracts for bacteria, *Planta Med.*, 1998, **64**, 711–713.
- 41 A. H. Abdelmonsef, *et al.*, Identification of Novel Antagonists for Rab38 Protein by Homology Modeling and Virtual Screening, *Comb. Chem. High Throughput Screening*, 2016, **19**, 1–18.
- 42 I. A. Shehadi, H. R. M. Rashdan and A. H. Abdelmonsef, Homology Modeling and Virtual Screening Studies of Antigen MLAA-42 Protein: Identification of Novel Drug Candidates against Leukemia—An *In Silico* Approach, *Comput. Math. Methods Med.*, 2020, **2020**, 8196147.
- 43 N. M. O'Boyle, *et al.*, Open Babel: An Open chemical toolbox, *J. Cheminf.*, 2011, **3**, 33.
- 44 S. Dallakyan and A. J. Olson, Small-Molecule Library Screening by Docking with PyRx, in *Chemical Biology*, Springer, 2015, vol. 1263, pp. 243–250.